

# On the analytical Solution of axisymmetric stagnation flow towards a shrinking sheet

M. Rahimpour, S. R. Mohebpour, A. Kimiaefar and G. H. Bagheri

**Abstract**—In this paper, an analytical solution for the axisymmetric stagnation point flow of a viscous and incompressible fluid, toward a shrinking sheet is presented. A similarity transformation reduces the Navier–Stokes equations to a set of non-linear ordinary differential equations which are solved analytically by means of Homotopy Analysis Method (HAM). The results obtained in this study are compared with numerical results released in the literature. Close agreement of the two sets of results indicates the accuracy of the HAM. The method can obtain an expression which is acceptable for all values of effective parameters and also is able to control the convergence of the solution.

**Keywords**—Analytical Solution, Axisymmetric Stagnation Flow, Homotopy Analysis Method (HAM), Shrinking Sheet.

## I. INTRODUCTION

**S**TAGNATION flow, describing the fluid motion near the stagnation region, exists on all solid bodies moving in a fluid. The stagnation region encounters the highest pressure, the highest heat transfer and the highest rate of mass deposition [1]. Problems such as the extrusion of polymers in melt-spinning processes, glass blowing, the continuous casting of metals, and the spinning of fibers all involve some aspect of flow over a stretching sheet or cylindrical fiber [2]. In stagnation point flow, rigid wall or a stretching or shrinking surface occupies the entire horizontal  $x$ -axis, the fluid domain is  $y > 0$  and the flow impinges on the wall with different origin of stretching or shrinking on the sheet.

Homman [3] was first to study axisymmetric stagnation flows. He introduced similarity transforms which reduced the Navier-Stokes equations to non-linear ordinary equations. Temperature distribution was later discussed by Sibulkin [4]. Wang [5] presented a similarity solution for an axisymmetric flow to a stretching sheet. Chiam [6] and Mahapatra and

Gupta [7], [8] considered stagnation flow on a stretching sheet. Wang [1] studied the flow pattern and temperature distribution in stagnation flow on a shrinking sheet. He showed that the non-alignment of the stagnation flow and the shrinking sheet complicates the flow structure. In these analyses, the governing equations were solved by numerical methods.

Analytical methods were used to study the viscous flow near a stagnation point. Xu *et al.* [9] studied the unsteady boundary layer flows of non-Newtonian fluids near a forward stagnation point. Hayat *et al.* [10], [11] investigated the MHD stagnation point flow of an upper convected Maxwell fluid over a stretching surface and MHD flow of a micropolar fluid near a stagnation point towards a non-linear stretching surface. Nazar *et al.* [12] studied the unsteady mixed convection boundary layer flow near the stagnation point on a vertical surface in a porous medium. Priede *et al.* [13] matched asymptotic solution for the solute boundary layer in a converging axisymmetric stagnation point flow. Ayub *et al.* [14] presented an analytical solution of stagnation-point flow of a viscoelastic fluid towards a stretching surface.

Most scientific problems in fluid mechanics and heat transfer are inherently nonlinear. Except a limited number of these problems, most of them do not have analytical solutions. Therefore, these nonlinear equations should be solved using other methods. Some of them are solved using numerical techniques and some are solved using perturbation method [15]. In the numerical method, stability and convergence should be considered so as to avoid divergence or inappropriate results. On the other hand in the numerical methods, the problem should be solved for each value of the effective parameters, which is deficiency of these methods. In the perturbation method, a small parameter is inserted in the equation. Therefore, finding the small parameter and exerting it into the equation are deficiencies of this method.

One of the semi-exact methods which do not need small/large parameters is the Homotopy Analysis Method (HAM), first proposed by Liao in 1992 [16], [17]. In this method the convergence region can be adjusted and controlled and it is the most important feature of this technique in comparison to other techniques. It should be emphasized that the Homotopy Perturbation Method (HPM) introduced in 1998 is only a special case of HAM [18], [19].

Up to now, no investigation has been made which provides the analytical solution for the axisymmetric stagnation flow towards a shrinking sheet. In this study, HAM is applied to

Manuscript received February 8, 2008; Revised version received April 8, 2008.

M. Rahimpour is with the Department of Mechanical Engineering, Shahid Bahonar University of Kerman, Kerman, Iran (e-mail: rahimpour@pasteur.ac.ir and mostafa\_rahimpour@yahoo.com).

S. R. Mohebpour is with the Department of Mechanical Engineering, Persian Gulf University, Bushehr, Iran (e-mail: srmohebpour@yahoo.com).

A. Kimiaefar is with the Department of Mechanical Engineering, Shahid Bahonar University of Kerman, Kerman, Iran (corresponding author to provide phone: +98 917 710 3873; fax: +98 341 2120964; e-mail: a.kimiaei@gmail.com).

G. H. Bagheri is with the Department of Mechanical Engineering, Shahid Bahonar University of Kerman, Kerman, Iran (e-mail: gh\_baghei@yahoo.com).

find an analytical solution of nonlinear ordinary differential equations arising from the similarity solution, and the results were compared with those obtained in [1]. Moreover the numerical solution based on shooting method and fourth order Runge Kutta method have been developed by authors of this article.

Fig. 1 shows an axisymmetric stagnation flow towards an axisymmetric shrinking sheet. Non alignment occurs when the line of symmetry of the stagnation flow and that of shrinking sheet are not matched.

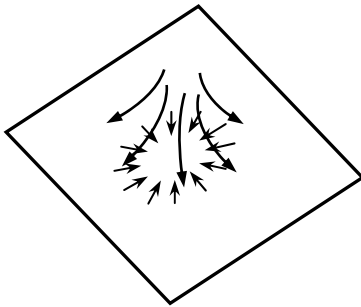


Fig. 1 Axisymmetric stagnation flow on a axisymmetric shrinking sheet

## II. MATHEMATICAL FORMULATIONS

Let  $(u, v, w)$  be the velocity components in the Cartesian coordinates  $(x, y, z)$ , respectively. For three dimensional incompressible flows, the continuity equation reduces to:

$$\frac{\partial u}{\partial x} + \frac{\partial v}{\partial y} + \frac{\partial w}{\partial z} = 0. \quad (1)$$

Wang [1] defined the following similarity transforms:

$$u = axf'(\eta) + bch(\eta), \quad v = ayf'(\eta), \quad w = -2\sqrt{va}f(\eta), \quad (2)$$

$$\eta = z\sqrt{a/v}, \quad (3)$$

where  $a > 0$  is the strength of the stagnation flow and is proportional to the free stream velocity far away from the shrinking (stretching) surface,  $b$  is the shrinking rate ( $b < 0$ ) or stretching rate ( $b > 0$ ) and  $-c$  is the location of the stretching origin and  $v$  is the kinematic viscosity.  $\eta$  is independent dimensionless parameter and primes denote differentiation with respect to  $\eta$ .  $f(\eta)$  and  $h(\eta)$  are the velocity similarity variables.

On the shrinking (stretching) surface the velocities are:

$$u_w = b(x+c), \quad v_w = \alpha ay, \quad w_w = 0, \quad (4)$$

where  $\alpha = b/a$ , is the ratio of the stretching rate to the strength of the stagnation flow. Wang [1] found that the solution is unique for  $\alpha \geq -1$  and there is no solution for

$\alpha < -1$ . This paper presents an analytical solution in the range of  $\alpha > -1$ .

The Navier–Stokes equations are reduced by using (2) and (3):

$$f''' + 2ff'' + 1 - f'^2 = 0, \quad (5)$$

$$h'' + 2fh' - hf' = 0. \quad (6)$$

The boundary conditions:

$$f(0) = 0, \quad f'(0) = b/a = \alpha, \quad f'(\infty) = 1, \quad (7)$$

$$h(0) = 1, \quad h(\infty) = 0. \quad (8)$$

Stream function for non-alignment flow ( $c \neq 0$ ) does not exist and fluid structure is completely three dimensional [1].

Once the velocities are known from the previous analysis, the temperatures can be found from the energy equation. A similarity solution exists [20] if the sheet and stream temperatures,  $T_0$  and  $T_\infty$ , are constant.

The three dimensional energy equation is written as:

$$u \frac{\partial T}{\partial x} + v \frac{\partial T}{\partial y} + w \frac{\partial T}{\partial z} = \kappa \left( \frac{\partial^2 T}{\partial x^2} + \frac{\partial^2 T}{\partial y^2} + \frac{\partial^2 T}{\partial z^2} \right), \quad (9)$$

here  $T$  is the temperature and  $\kappa$  is the thermal diffusivity. A dimensionless temperature  $\theta$  is defined;

$$\theta = \frac{T - T_\infty}{T_0 - T_\infty}. \quad (10)$$

The energy equation (9) becomes:

$$\theta''(\eta) + 2Pr f(\eta)\theta'(\eta) = 0, \quad (11)$$

where  $Pr = v/\kappa$  is the Prandtl number. The boundary conditions are:

$$\theta(0) = 1, \quad \theta(\infty) = 0. \quad (12)$$

It is of interest to obtain the value of  $-\theta'(0)$  which is an effective parameter for the heat transfer.

## III. HAM SOLUTIONS

The governing equations for the stagnation flow towards a axisymmetric shrinking sheet are expressed by (5) and (6). Nonlinear operators are defined as follows:

$$N_f[f(\eta, q)] = \frac{\partial^3 f(\eta, q)}{\partial \eta^3} + 2f(\eta, q) \frac{\partial^2 f(\eta, q)}{\partial \eta^2} - \left( \frac{\partial f(\eta, q)}{\partial \eta} \right)^2 + 1, \quad (13)$$

$$N_h[h(\eta, q)] = \frac{\partial^2 h(\eta, q)}{\partial \eta^2} - h(\eta, q) \frac{\partial f(\eta, q)}{\partial \eta} + 2f(\eta, q) \frac{\partial h(\eta, q)}{\partial \eta}, \quad (14)$$

where  $q \in [0, 1]$  is the embedding parameter. As the embedding parameter increases from 0 to 1,  $U(\eta, q)$  and  $Y(\eta, q)$  vary from the initial guess,  $U_0(\eta)$  and  $Y_0(\eta)$ , to the exact solution,  $U(\eta)$  and  $Y(\eta)$ :

$$f(\eta, 0) = U_0(\eta), \quad f(\eta, 1) = U(\eta), \quad (15)$$

$$h(\eta, 0) = Y_0(\eta), \quad h(\eta, 1) = Y(\eta). \quad (16)$$

Expanding  $f(\eta, q)$  in Taylor series with respect to  $q$  leads to:

$$f(\eta, q) = U_0(\eta) + \sum_{m=1}^{\infty} U_m(\eta) q^m, \quad (17)$$

$$h(\eta, q) = Y_0(\eta) + \sum_{m=1}^{\infty} Y_m(\eta) q^m, \quad (18)$$

where

$$U_m(\eta) = \left. \frac{1}{m!} \frac{\partial^m f(\eta, q)}{\partial q^m} \right|_{q=0}, \quad (19)$$

$$Y_m(\eta) = \left. \frac{1}{m!} \frac{\partial^m h(\eta, q)}{\partial q^m} \right|_{q=0}. \quad (20)$$

Homotopy analysis method can be expressed by many different base functions [17]; according to the governing equations, it is straightforward to use a base function in the form of:

$$U(\eta) = \sum_{m=1}^{\infty} \sum_{p=1}^{\infty} b_{pm} \eta^p e^{-m\eta}, \quad (21)$$

$$Y(\eta) = \sum_{m=1}^{\infty} \sum_{p=1}^{\infty} d_{pm} \eta^p e^{-m\eta}. \quad (22)$$

$b_{pm}$  and  $d_{pm}$  are the coefficients should be determined. When the base function is selected, the auxiliary functions  $H_f(\eta)$  and  $H_h(\eta)$ , initial approximations  $U_0(\eta)$ ,  $Y_0(\eta)$  and the auxiliary linear operators  $L_f$  and  $L_h$  must be chosen in such a way that the corresponding high-order deformation equations have solutions with the functional form similar to the base functions. It is worth mentioning that the presence of

expressions such as  $\eta^n \sin(m\eta)$  prevents the convergence of the analytical solution. This method is known as *the rule of solution expression* [17]. The linear operators are chosen as:

$$L_f[f(\eta, q)] = \frac{\partial^3 f(\eta, q)}{\partial \eta^3} + \frac{\partial^2 f(\eta, q)}{\partial \eta^2}, \quad (23)$$

$$L_h[h(\eta, q)] = \frac{\partial^2 h(\eta, q)}{\partial \eta^2} - h(\eta, q). \quad (24)$$

Equations (23) and (24) lead to:

$$L_f[c_1 + c_2\eta + c_3e^{-\eta}] = 0, \quad (25)$$

$$L_h[c_4 + c_5e^{-\eta}] = 0, \quad (26)$$

where  $c_1$  to  $c_5$  are the integral constants.

According to *the rule of solution expression* and the initial conditions, the initial approximations,  $U_0$  and  $Y_0$  as well as the integral constants,  $c_1$  to  $c_5$ , are formed as:

$$U_0(\eta) = c_1 + c_2\eta + c_3e^{-\eta}, \quad c_3 = 1 - \alpha, \quad c_2 = 1, \quad c_1 = -c_3, \quad (27)$$

$$Y_0(\eta) = c_4 + c_5e^{-\eta}, \quad c_4 = 0, \quad c_5 = 1. \quad (28)$$

The zero<sup>th</sup> order deformation equation and its boundary conditions for  $f(\eta)$  and  $h(\eta)$  are:

$$(1-q)L_f[f(\eta, q) - U_0(\eta)] = q\hbar H_f(\eta) N_f[f(\eta, q)], \quad (29)$$

$$f(0, q) = 0, \quad \frac{\partial f(0, q)}{\partial \eta} = \alpha, \quad \frac{\partial f(\infty, q)}{\partial \eta} = 1, \quad (30)$$

$$(1-q)L_h[h(\eta, q) - Y_0(\eta)] = q\hbar N_h[h(\eta, q)], \quad (31)$$

$$h(0, q) = 1, \quad h(\infty, q) = 0, \quad (32)$$

$\hbar \neq 0$  is a nonzero auxiliary parameter. According to *the rule of solution expression* and from (29), the auxiliary functions

$H_f(y)$  can be chosen as follows:

$$H_f(y) = y^p e^{-ry}. \quad (33)$$

Differentiating (29), and (30),  $m$  times, with respect to the embedding parameter  $q$  and then setting  $q = 0$  in the final expression and dividing it by  $m!$ , reduced to:

$$U_m(\eta) = \hbar \int_0^\eta \int_0^\eta \int_0^\eta H_f(\eta) e^\eta R_m(U_{m-1}) d\eta d\eta d\eta + \chi_m U_{m-1}(\eta) + c_1 + c_2 \eta + c_3 e^{-\eta}, \quad (34)$$

$$U_m(0) = 0, \quad U'_m(0) = 0, \quad U'_m(\infty) = 0, \quad (35)$$

$$Y_m(\eta) = \frac{1}{2} \hbar e^\eta \left( \int_0^\eta e^{-\eta} R_m(Y_{m-1}) d\eta - \int_0^\eta e^\eta R_m(Y_{m-1}) d\eta \right) + \chi_m Y_{m-1}(\eta) + c_4 e^{-\eta} + c_3 e^\eta, \quad (36)$$

$$Y_m(0) = 0, \quad Y_m(\infty) = 0. \quad (37)$$

Equations (34) and (36) are the  $m^{\text{th}}$  order deformation equation for  $f(\eta)$  and  $h(\eta)$ , where:

$$R_m(U_{m-1}) = \chi_m 1 + \frac{d^3 U_{m-1}(\eta)}{d\eta^3} + \left( \sum_{z=0}^{m-1} U_z(\eta) \frac{d^2 U_{m-1-z}(\eta)}{d\eta^2} \right) - \left( \sum_{z=0}^{m-1} \frac{dU_z(\eta)}{d\eta} \frac{dU_{m-1-z}(\eta)}{d\eta} \right), \quad (38)$$

$$R_m(Y_{m-1}) = \frac{d^2 Y_{m-1}(\eta)}{d\eta^2} + 2 \left( \sum_{z=0}^{m-1} U_z(\eta) \frac{dY_{m-1-z}(\eta)}{d\eta} \right) - \left( \sum_{z=0}^{m-1} Y_{m-1-z}(\eta) \frac{dU_{m-1-z}(\eta)}{d\eta} \right), \quad (39)$$

$$\chi_m = \begin{cases} 0, & m \leq 1 \\ 1, & m > 1 \end{cases} \quad (40)$$

The rate of convergence can be increased when suitable values are selected for  $p$  and  $r$ . According to the rule of solution expression the suitable values for  $p$  and  $r$  are  $\{p = 0, r = 1\}$ .

Consequently, the corresponding auxiliary functions were determined as  $H_f(\eta) = e^{-\eta}$ . As a result of this selection, the solution's series  $U(\eta)$  and  $Y(\eta)$  is developed up to 20<sup>th</sup> order of approximation, so  $f(\eta)$  and  $h(\eta)$  is obtained as follows:

$$f(\eta) = U_0(\eta) + \sum_{m=1}^{20} U_m(\eta) q^m \Big|_{q=1} = U_0(\eta) + U_1(\eta) + \dots = (\alpha - 1) + \eta + (1 - \alpha)e^{-\eta} - \hbar(-\alpha^2 - 3e^{-\eta} + 2e^{-\eta}\alpha^2 + 2e^{-\eta}\alpha^2 + 2e^{-2\eta} + 2e^{-2\eta}\eta - e^{-2\eta}\alpha^2 - \alpha e^{-2\eta}\eta - \alpha e^{-2\eta} + 1 + e^{-\eta}\alpha)/4 + \dots \quad (41)$$

$$h(\eta) = Y_0(\eta) + \sum_{m=1}^{20} Y_m(\eta) q^m \Big|_{q=1} = Y_0(\eta) + Y_1(\eta) + \dots = e^{-\eta} \frac{1}{6} \hbar e^{-\eta} (2 - 3\eta - 2e^{-\eta} + 2e^{-\eta}\alpha + 6\alpha\eta + 3\eta^2 - 2\alpha) + \dots \quad (42)$$

$\theta(\eta)$  has an analytical solution as follows:

$$\theta(\eta) = C_1 + C_2 \int e^{-2\text{Pr} \int f(\eta) d\eta} d\eta. \quad (43)$$

The HAM solution can be applied to obtain the temperature distribution as follows:

$$N_h[\theta(\eta, q)] = \frac{\partial^2 \theta(\eta, q)}{\partial \eta^2} + 2\text{Pr} f(\eta, q) \frac{\partial \theta(\eta, q)}{\partial \eta}, \quad (44)$$

$$(1 - q) L_q[\theta(\eta, q) - Q_0(\eta)] = q \hbar N_h[\theta(\eta, q)], \quad (45)$$

$$\theta(0, q) = 1, \quad \theta(\infty, q) = 0. \quad (46)$$

The  $m^{\text{th}}$  order deformation equation for  $m \geq 1$  are:

$$Q_m(\eta) = \frac{1}{2} \hbar e^\eta \left( \int_0^\eta e^{-\eta} R_m(Q_{m-1}) d\eta - \int_0^\eta e^\eta R_m(Q_{m-1}) d\eta \right) + \chi_m Q_{m-1}(\eta) + c_4 e^{-\eta} + c_3 e^\eta, \quad (47)$$

$$Q_m(0) = 0, \quad Q_m(\infty) = 0, \quad (48)$$

where:

$$R_m(Q_{m-1}) = \frac{d^2 Q_{m-1}(\eta)}{d\eta^2} + 2\text{Pr} \left( \sum_{z=0}^{m-1} U_z(\eta) \frac{dQ_{m-1-z}(\eta)}{d\eta} \right). \quad (49)$$

The solution's series  $Q(\eta)$  is developed up to 20<sup>th</sup> order of approximation.

$$\theta(\eta) = Q_0(\eta) + \sum_{m=1}^{20} Q_m(\eta) q^m \Big|_{q=1} = Q_0(\eta) + Q_1(\eta) + \dots = e^{-\eta} + \frac{1}{6} \hbar e^{-\eta} (-4\text{Pr}\alpha + 4\text{Pr} - 3\text{Pr}\eta - 4e^{-\eta}p + 4e^{-\eta}p\alpha - 3\eta + 6\text{Pr}\alpha\eta + 3\text{Pr}\eta^2 \dots) \quad (50)$$

#### IV. CONVERGENCE OF HAM SOLUTION

The analytical solution should converge. It should be noted that the auxiliary parameter  $\hbar$ , as pointed out by Liao [17], controls the convergence and accuracy of the solution series. In order to define a region where the solution series is independent on  $\hbar$ , a multiple of  $\hbar$ -curves are plotted. The region where the distribution of  $f''$ ,  $f'$ ,  $f$  and  $h'$ ,  $h$  and

$\theta'$ ,  $\theta$  versus  $\hbar$  is a horizontal line is known as the convergence region for the corresponding function. The common region among the  $f(\eta)$  and its derivatives,  $h(\eta)$  and its derivative and  $\theta(\eta)$  and its derivative are known as the overall convergence region.

To study the influence of  $\hbar$  on the convergence of solution, the  $\hbar$ -curve of  $f''(0)$ ,  $f'(1)$ ,  $f(2)$  and  $h'(0)$ ,  $h(1)$  and  $\theta'(0)$ ,  $\theta(1)$  are plotted by 15<sup>th</sup> order approximation of solution for selected  $\alpha$ , as shown in Fig. 2. Moreover, increasing the order of approximation increases the range of the convergence region, as shown in Fig. 3.

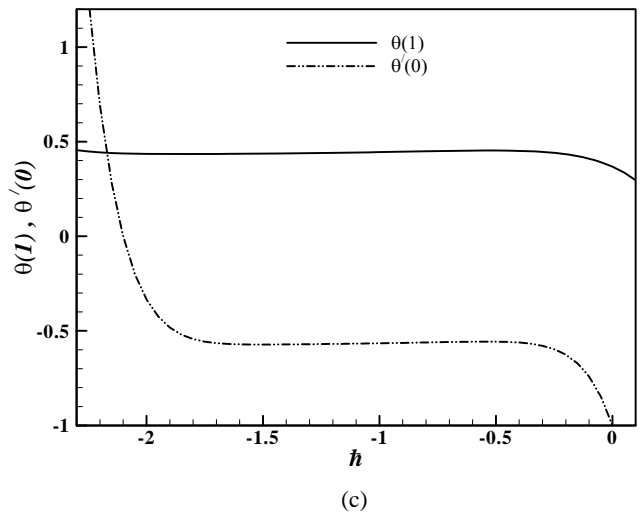
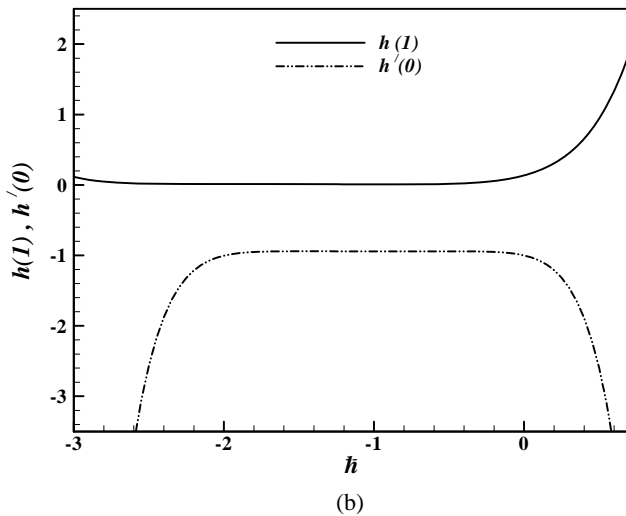
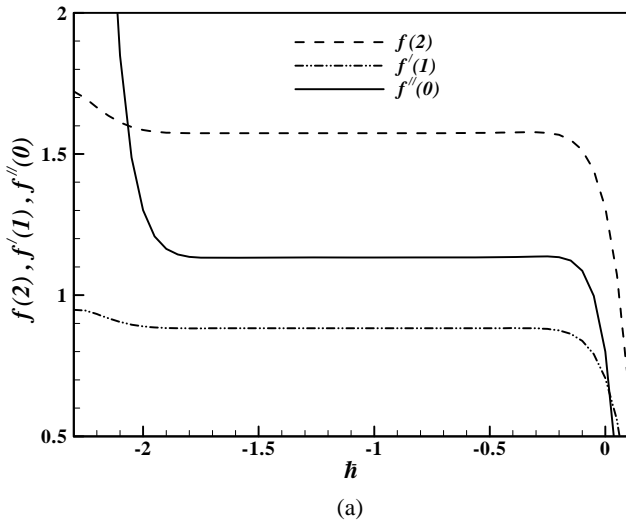
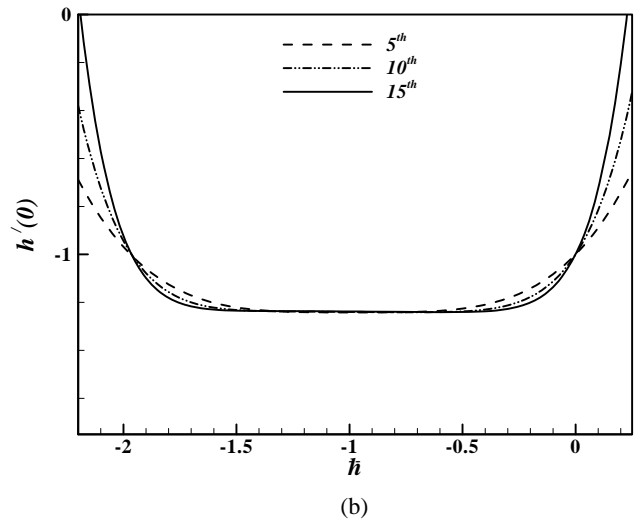
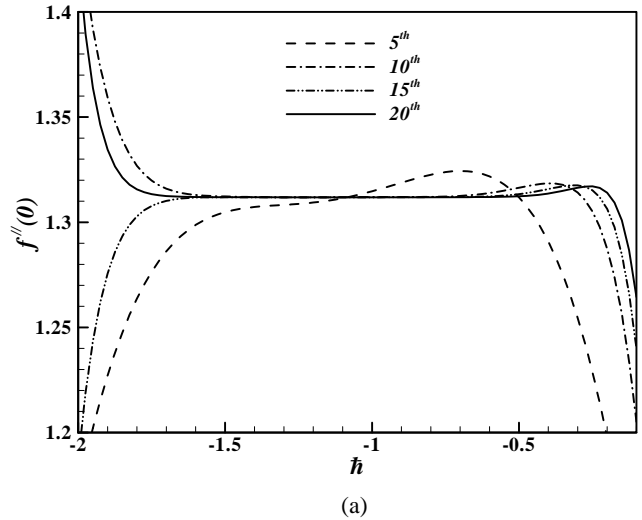


Fig. 2 The  $\hbar$ -curves to indicate the convergence region: (a)  $\alpha = 0.2$  ; (b)  $\alpha = 0$  ; (c)  $\alpha = -0.25$ ,  $Pr = 0.7$  .



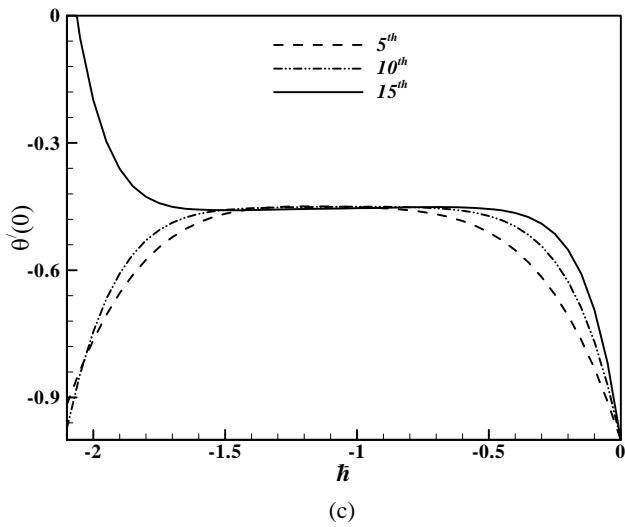


Fig. 3 The effect of order of approximation on convergence region. (a)  $f''(0)$ ,  $\alpha = 0$ ; (b)  $h'(0)$ ,  $\alpha = 0.5$ ; (c)  $\theta'(0)$ ,  $\alpha = -0.5$ ,  $Pr = 0.7$ .

V. RESULTS AND DISCUSSION

Equations (6), (7) and (12) along with the boundary

Table I Comparing the present analytical and numerical results for  $f''(0)$  with the results of [1].

$\alpha$	$f''(0)$					[1]
	5 <sup>th</sup> order	10 <sup>th</sup> order	15 <sup>th</sup> order	20 <sup>th</sup> order	Numeric.	
-0.95	1.02080507	0.98798215	0.96263402	0.946815	0.94688120	0.9469
-0.75	1.37582656	1.35311884	1.35300321	1.35285011	1.35285001	1.35284
-0.5	1.49218863	1.49006144	1.48999537	1.49002102	1.49000996	1.49001
-0.25	1.45635226	1.45651781	1.45655385	1.45659894	1.45659973	1.45664
0	1.32856195	1.31186085	1.31187102	1.31193770	1.31193769	1.311938
0.1	1.22883485	1.22931217	1.22899112	1.22911310	1.22911275	1.22911
0.2	1.13347782	1.13368023	1.13355123	1.13373987	1.13374336	1.13374
0.5	0.78069662	0.78024735	0.78026471	0.78032334	0.78032335	0.78032
1	0	0	0	0	0	0
2	-2.13267341	-2.13196947	-2.13082815	-2.13107410	-2.13106966	-2.13107
5	-11.51664341	-11.73022468	-11.795058010	-11.80221341	-11.80221358	-11.8022

Table II Comparing the present analytical and numerical results for  $h'(0)$  with the results of [1].

$\alpha$	$h'(0)$					[1]
	5 <sup>th</sup> order	10 <sup>th</sup> order	15 <sup>th</sup> order	Numeric.		
-0.95	0.2319867	0.2712571	0.2684487	0.2684501	0.26845	0.26845
-0.75	-0.2306214	-0.2221852	-0.2207901	-0.2207899	-0.22079	-0.22079
-0.5	-0.5387551	-0.5351514	-0.5323681	-0.5323711	-0.53237	-0.53237
-0.25	-0.8450057	-0.7905277	-0.7563891	-0.7563901	-0.75639	-0.75639
0	-0.9433567	-0.9430505	-0.9387311	-0.9387315	-0.93873	-0.93873
0.1	-1.0090467	-1.0080904	-1.0039871	-1.0040260	-1.004	-1.004
0.2	-1.0710228	-1.0696988	-1.0658870	-1.0659335	-1.0659	-1.0659
0.5	-1.2400660	-1.2391778	-1.2355030	-1.2354515	-1.2355	-1.2355
1	-1.4878204	-1.4838635	-1.4793212	-1.4793376	-1.4793	-1.4793
2	-1.8959174	-1.8908089	-1.8799812	-1.8799488	-1.88	-1.88
5	-2.7587690	-2.7777899	-2.7616891	-2.7617243	-2.7617	-2.7617

conditions (7), (8) and (12) are solved using HAM for some values of the parameter  $\alpha$ . The rate of convergency and results for  $f''(0)$  and  $h'(0)$  at some values of  $\alpha$  are shown in Table I and Table II respectively. The results obtained from HAM solution are compared with results of [1]. The same comparison is made with the results of numerical solution of similarity equations based on fourth order Runge Kutta method, developed by these authors.

The results show that HAM gives an analytical solution with high order of accuracy with a few iterations.

Variations of the  $f''(0)$  and  $h'(0)$  relative to the  $\hbar$  are presented in Table III and Table IV, show that results are independent from  $\hbar$  in convergence region.

Table III Variation of the  $f''(0)$  in the convergence region with 20<sup>th</sup> order approximation.

$f''(0)$					
$\alpha$	$\hbar$	HAM	$\hbar$	HAM	[1]
-0.95	-1.6	0.9457240	-0.4	0.9455352	0.9469
-0.75	-1.7	1.3524837	-0.6	1.3529858	1.35284
-0.5	-1.8	1.4900097	-0.6	1.4900624	1.49001
-0.25	-1.8	1.4566012	-0.6	1.4565778	1.45664
0	-1.8	1.3119512	-0.6	1.3118981	1.311938
0.1	-1.8	1.2291474	-0.6	1.2284004	1.22911
0.2	-1.7	1.1337501	-0.6	1.1336301	1.13374
0.5	-1.6	0.7803720	-0.4	0.7802590	0.78032
2	-0.7	-2.1310722	-0.2	-2.1317621	-2.13107
5	-0.6	-11.8021978	-0.1	-11.8023868	-11.8022

Table IV Variation of the  $h'(0)$  in the convergence region with 20<sup>th</sup> order approximation.

$h'(0)$					
$\alpha$	$\hbar$	HAM	$\hbar$	HAM	[1]
-0.95	-1.5	0.268435	-0.4	0.268439	0.26845
-0.75	-1.6	-0.220778	-0.5	-0.220780	-0.22079
-0.5	-1.6	-0.532349	-0.6	-0.532357	-0.53237
-0.25	-1.7	-0.756376	-0.6	-0.756380	-0.75639
0	-1.7	-0.938729	-0.8	-0.938727	-0.93873
0.1	-1.7	-1.003832	-0.6	-1.003874	-1.004
0.2	-1.7	-1.065775	-0.6	-1.065698	-1.0659
0.5	-1.7	-1.235632	-0.6	-1.235641	-1.2355
1	-1.6	-1.479223	-0.4	-1.479211	-1.4793
2	-1.6	-1.881134	-0.4	-1.881582	-1.88
5	-1.5	-2.761812	-0.4	-2.761801	-2.7617

Fig. 4 is prepared in order to see the effects of  $\alpha$  on the velocity components  $f'(\eta)$ ,  $f(\eta)$  and  $h(\eta)$ .

Fig. 6 shows dimensionless temperature distribution in the flow domain for various values of  $\alpha$ . It's obvious that as  $\alpha$  increases, thermal boundary layer thickness decreases. Also decreasing the Prandtl number increases the thermal boundary layer thickness.

$-\theta'(0)$  is an important parameter for heat transfer. Since there is an analytical solution for  $f(\eta)$ , obtained from HAM, the  $-\theta'(0)$  can be found from two different ways; the HAM and equation (43) which can be reduced to:

$$-\theta'(0) = \frac{1}{\int_0^\infty e^{-2Pr \int_0^\eta f d\eta} d\eta} \tag{51}$$

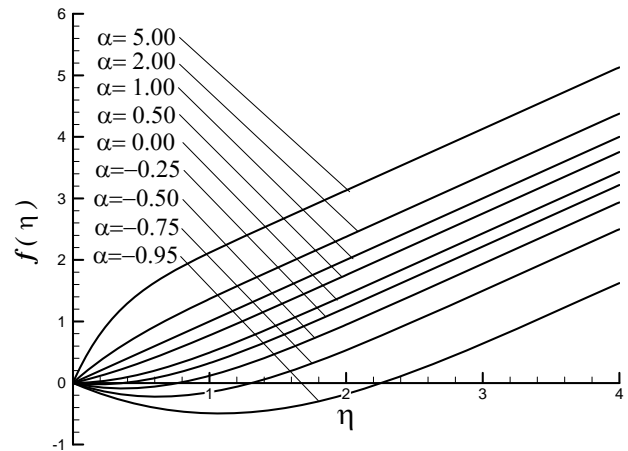
By integrating (51) using numerical methods (The Simpson's 3/8 Rule),  $-\theta'(0)$  can simply be estimated. The HAM results shown in Table V and Table VI indicated that shrinking sheet has lower values of  $-\theta'(0)$  as compared to stretching sheet.  $-\theta'(0)$  lessens at the same Prandtl number

when  $\alpha$  is decreased.

In the case of  $\alpha$  approaching zero, stagnation flow on the sheet becomes similar to the stagnation flow studied by Homman [3] and Sibulkin [4]. Table VII shows the comparison between HAM results and numerical solution from [20]. A general equation is obtained from HAM which is acceptable for all values of  $\alpha$  and Prandtl number:

$$-\theta'(0) = -0.367\alpha Pr - 1.3 \times 10^{-3} \alpha^2 Pr^2 + 3.59 \times 10^{-4} \alpha^3 Pr^2 + 3.275 \times 10^{-7} \alpha^4 Pr - 1.887 \times 10^{-4} \alpha^4 Pr^2 + 6.818 \times 10^{-5} \alpha^5 Pr^2 + 5.21 \times 10^{-5} \alpha^6 Pr^2 - 7.64 \times 10^{-5} \alpha^7 Pr^2 + 2.64 \times 10^{-5} \alpha^9 Pr^2 - 3.58 \times 10^{-6} \alpha^{11} Pr^2 + 4.97 \times 10^{-7} \alpha^{12} Pr^2 + \dots \tag{52}$$

This solution was obtained by 10<sup>th</sup> order approximation for  $\theta(\eta)$  and 10<sup>th</sup> order approximation for  $f(\eta)$  with  $\hbar = -1.1$ .



(a)

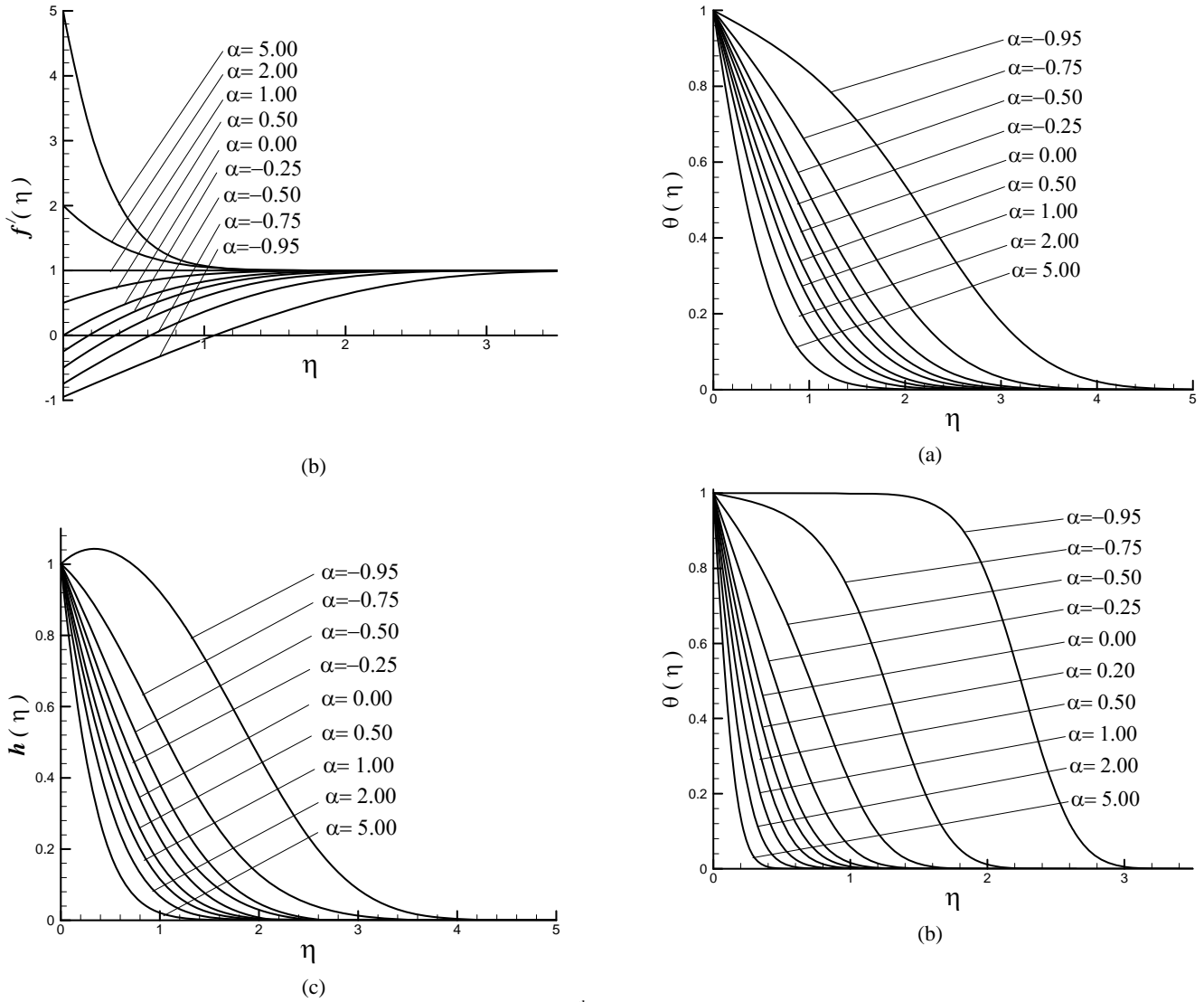


Fig. 4 Velocity components predicted by the HAM solution with 20<sup>th</sup> order approximation: (a) the function  $f(\eta)$  ; (b) the function  $f'(\eta)$  ; and (c) the function  $h(\eta)$  .

Fig. 5 Temperature distributions predicted by the HAM solution with 20<sup>th</sup> order approximation: (a)  $Pr = 0.7$  ; (b)  $Pr = 7.0$  .

Table V Variations of  $-\theta'(0)$  with respect to  $Pr$  for the axisymmetric stretching sheet ( $\alpha \geq 0$ ) .

		$-\theta'(0)$							
		$\alpha$	0	0.1	0.2	0.5	1	2	5
Pr=0.7	HA		0.66540000	0.69830000	0.72970000	0.81676798	0.94406979	1.15706992	1.63771881
	M (51)		0.66537763	0.69830523	0.72974134	0.81678146	0.94406979	1.15711096	1.63677035
Pr=7.0	HA		1.54570000	1.72280000	1.89040000	2.34510969	2.98541099	4.00505277	6.19312765
	M (51)		1.54577945	1.72284802	1.89041135	2.34511860	2.98541099	4.00496580	6.16452790

Table VI Variations of  $-\theta'(0)$  with respect to  $Pr$  for the axisymmetric shrinking sheet ( $\alpha < 0$ ) .

$-\theta'(0)$				
$\alpha$	-0.25	-0.5	-0.75	-0.95

Pr=0.7	HAM	0.57485972	0.46709271	0.32600021	0.13688695
	(51)	0.57483466	0.46707156	0.32592005	0.13685381
Pr=7.0	HAM	1.05649153	0.51204057	0.07191553	0.00003548
	(51)	1.05647092	0.51202490	0.07190343	0.00003896

Table VII Comparing the results of present analytical solution for  $-\theta'(0)$  with [20].

Pr	$-\theta'(0)$					
	0.01	0.1	1	10	100	1000
HAM	0.1062	0.30154	0.7622	1.752	3.8702	8.4267
[20]	0.106	0.301	0.762	1.752	3.87	8.427

Note that, as pointed in [18] and [19], the results given by the ‘‘Homotopy Perturbation Method’’ are exactly the same as those given by the HAM when  $\hbar = -1$  and  $H(\eta) = 1$ , because the ‘‘Homotopy Perturbation Method’’ is only a unique case of the HAM. The comparison between HAM and HPM for  $f''(0)$  is shown in Fig. 7. The figure shows that for  $\alpha < 2$ , the prediction of the two methods are identical, and when  $\alpha$  is increase ( $\alpha \geq 2$ ), the deviation between two methods becomes more significant, because the HPM solution gets divergent.

### I. CONCLUSION

The nonlinear differential equations resulting from similarity solution of stagnation flow towards a shrinking sheet is studied using Homotopy Analysis Method (HAM). The comparison between numerical results and convergence study shows that using approximations of small orders, results in satisfactory accuracy and increasing the order of approximation, the accuracy is increased. After demonstrating its effectiveness as a powerful analytical technique, the effects of different parameters such as the shrinking rate, non-alignment shrinking and Prandtl number on the velocity distribution and temperature distribution are presented.

The proposed analytical approach has many applications, and thus may be applied in similar ways to other boundary-layer flows to get accurate series solutions.

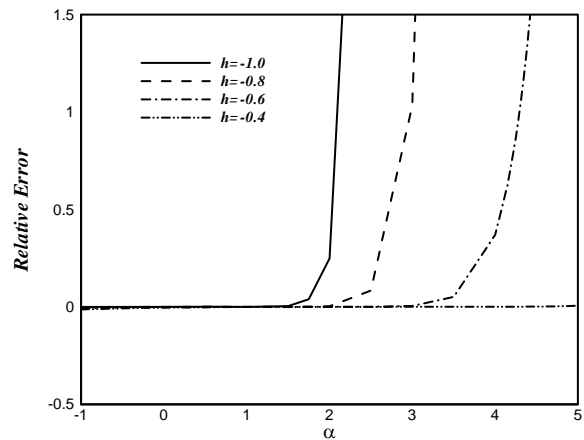


Fig. 6 Comparing the results of  $f''(0)$  predicted by the HAM and HPM. (Relative Error defined as:  $\frac{f''(0)_{Numeric} - f''(0)_{HAM}}{f''(0)_{Numeric}}$ )

### REFERENCES

- [1] C. Y. Wang, ‘‘Stagnation flow towards a shrinking sheet,’’ *Int. J. Non-Linear Mech.*, vol. 43, 2008, pp. 377–382.
- [2] J. Pualet and P. Weidman, ‘‘Analysis of stagnation point flow toward a stretching sheet,’’ *Int. J. Non-Linear Mech.*, vol. 42, 2008, pp. 1084–1091.
- [3] F. Homann, ‘‘Der einfluss grosser zahigkeit bei der stromung um den zylinder und um die kugel,’’ *Z. Angew. Math. Mech.*, vol. 16, 1936, pp. 153–164.
- [4] M. Sibulkin, ‘‘Heat transfer near the forward stagnation point of a body revolution,’’ *J. Aeronaut. Sci.*, vol. 19, 1952, pp. 570–571.
- [5] C. Y. Wang, ‘‘The three-dimensional flow due to a stretching flat surface,’’ *Phys. Fluids*, vol. 27, 1984, pp. 1915–1917.
- [6] T. C. Chiam, ‘‘Stagnation-point flow towards a stretching plate,’’ *J. Phys. Soc. Japan*, vol. 63, 1994, pp. 2443–2444.
- [7] T. R. Mahapatra and A. S. Gupta, ‘‘Heat transfer in stagnation-point flow towards a stretching sheet,’’ *J. Heat Mass Transfer*, vol. 38, 2002, pp. 517–521.
- [8] T. R. Mahapatra and A. S. Gupta, ‘‘Stagnation-point flow towards a stretching surface,’’ *Can. J. Chem. Eng.*, vol. 81, 2003, pp. 258–263.
- [9] H. Xu, S.J. Liao and I. Pop, ‘‘Series solution of unsteady boundary layer flows of non-Newtonian fluids near a forward stagnation point,’’ *J. Non-Newtonian Fluid Mech.*, vol. 139, 2006, pp. 31–43.
- [10] T. Hayat, Z. Abbas and M. Sajid, ‘‘MHD stagnation-point flow of an upper-convected Maxwell fluid over a stretching surface’’, *Chaos Solitons Fractals*, to be published.

- [11] T. Hayat, T. Javed and Z. Abbas, "MHD flow of a micropolar fluid near a stagnation-point towards a non-linear stretching surface," *Nonlinear Anal.: Real World Appl.* to be published.
- [12] R. Nazar, N. Amin and I. Pop, "Unsteady mixed convection boundary layer flow near the stagnation point on a vertical surface in a porous medium," *Int. J. Heat Mass Transfer*, vol. 47, 2004, pp. 2681–2688.
- [13] J. Priede and G. Gerbeth, "Matched asymptotic solution for the solute boundary layer in a converging axisymmetric stagnation point flow," *Int. J. Heat Mass Transfer*, vol. 50, 2007, pp. 216–225
- [14] M. Ayub, H. Zaman, M. Sajid and T. Hayat, "Analytical solution of stagnation-point flow of a viscoelastic fluid towards a stretching surface," *Commun. Nonlinear Sci. Numer. Simulat.*, vol. 13, 2008, pp. 1822–1835
- [15] A. H. Nayfeh, *Problems in Perturbation*. 2nd ed., N.Y.: John Wiley & Sons, 1993.
- [16] SJ. Liao, "The proposed homotopy analysis technique for the solution of nonlinear problems," Ph.D. dissertation, Shanghai Jiao Tong Univ., 1992.
- [17] SJ. Liao, *Beyond perturbation: introduction to the homotopy analysis method*. Boca Raton, FL.: Chapman & Hall/CRC Press, 2003.
- [18] SJ. Liao, "Comparison between the homotopy analysis method and homotopy perturbation method," *Appl. Math. Comput.*, vol. 169, 2005, pp. 1186–1194.
- [19] M. Sajid, T. Hayat and S. Asghar, "Comparison between the HAM and HPM solutions of thin film flows of non-Newtonian fluids on a moving belt," *Nonlinear Dynamics*, vol. 50, 2007, pp. 27–35.
- [20] F. M. White, *Viscous Fluid Flow*. 3th ed., Boston: McGraw-Hill, 2006.